**Chinese Journal of Health Management**
*Volume 20 Issue 3, Year of Publication 2026, Page 755-761 | DoI-10.564220/1674-0815.2026.97*

ISSN: 1674-0815

**Chinese Journal of Health Management**

Chinese Medical Association


# Stimuli-Responsive Green-Synthesized Iron Oxide Nanoparticles for Smart Drug Release in the Tumor Microenvironment

**Aakash Luniya, Rajendra, Vidhya Charan Pandey, Sonu Alam, Vishal Kumar, Kanaiya Kumar**
College of Pharmacy, Faculty of Medical and Paramedical Sciences, SAM Global University, Raisen, M. P., India

***Article Information***
Received: 17-12-2025
Revised: 22-01-2026
Accepted: 13-02-2026
Published: 29-03-2026

**Keywords**
*Green synthesis; Iron oxide nanoparticles; Tumor microenvironment; pH-responsive drug release; Doxorubicin; Folate targeting.*

## ABSTRACT:
Conventional cancer chemotherapy is limited by non-selective biodistribution, severe systemic toxicity and rapid clearance of free drugs. Stimuli-responsive nanocarriers that exploit the unique features of the tumor microenvironment (TME) — mildly acidic pH, redox imbalance and overexpressed surface receptors — represent a promising route to selective drug delivery. In this study, magnetite ($Fe_3O_4$) nanoparticles were green-synthesized using an aqueous *Moringa oleifera* leaf extract acting as a reductant and capping agent, surface-coated with chitosan, conjugated with folic acid (FA) for active targeting and loaded with doxorubicin (DOX) to obtain DOX-FA-CS-$Fe_3O_4$ nanoparticles. Comprehensive characterization (UV–Vis, FTIR, XRD, TEM, DLS and VSM) confirmed crystalline, spherical, superparamagnetic nanoparticles with a hydrodynamic diameter of 134.6 ± 8.2 nm, zeta potential of +28.4 ± 1.6 mV, drug-loading efficiency of 18.7 ± 1.1 % and encapsulation efficiency of 82.4 ± 2.3 %. The nanocarriers showed strong pH-dependent release: ~89.8 % of DOX was released at pH 5.0 versus only ~29.1 % at pH 7.4 over 72 h. In vitro cytotoxicity against MCF-7 breast cancer cells revealed an $IC_{50}$ of 3.42 µg $mL^{-1}$ for the formulation, while normal L929 fibroblasts retained > 70 % viability at 10 µg $mL^{-1}$, demonstrating selective tumor toxicity. The system thus offers an eco-friendly, biocompatible and TME-responsive platform for smart anticancer drug delivery.of encorafenib. Further in vivo studies would be useful to confirm their applicability in glioblastoma treatment.

## 1. INTRODUCTION:
Cancer remains one of the leading causes of mortality worldwide, with an estimated 19.3 million new cases and 10.0 million cancer-related deaths reported in 2020, and projections indicating a continued rise through 2040[1]. The most recent GLOBOCAN update for 2022 confirms breast, lung and colorectal cancers as the dominant contributors to this global burden[2]. Conventional chemotherapy, although effective in many regimens, is

hampered by non-specific cytotoxicity, dose-limiting side effects, multidrug resistance and rapid plasma clearance of small-molecule drugs[3,4]. Engineered nanoparticles (NPs) have therefore emerged as a transformative tool for cancer therapy, offering protection of payloads, prolonged circulation and the ability to accumulate preferentially in solid tumors via the enhanced permeability and retention (EPR) effect[5,6].

Despite the success of synthetic nanocarriers, traditional chemical and physical synthesis routes for inorganic NPs typically involve toxic reductants, organic solvents and high energy input that may compromise biocompatibility[7]. Green synthesis, particularly plant-mediated synthesis, has gained momentum as an environmentally benign, scalable and inexpensive alternative[7,8]. Phytochemicals such as polyphenols, flavonoids, terpenoids and reducing sugars present in plant extracts simultaneously reduce metal precursors and stabilize the resulting NPs through capping interactions, eliminating the need for hazardous reagents[9–11]. Among biogenic metal-oxide nanoparticles, iron oxide ($Fe_3O_4$) NPs are particularly attractive for cancer applications owing to their superparamagnetism, high saturation magnetization, magnetic-targeting capability and inherent biocompatibility[12–14].

Solid tumors generate a distinctive microenvironment characterized by mildly acidic extracellular pH (~6.5–6.8), severely acidic intracellular endo-lysosomal compartments (pH 4.5–5.5), elevated reactive oxygen species, overexpressed proteolytic enzymes, hypoxia and aberrant vasculature[15,16]. Although the EPR effect can drive a fraction of long-circulating nanoparticles into solid tumors, recent meta-analyses have shown that on average less than 1 % of an injected dose typically reaches the tumor, and burst leakage in plasma can substantially blunt the therapeutic index of cytotoxic payloads such as doxorubicin[33,34]. These limitations have catalyzed the design of carriers whose drug retention is high during circulation but switches abruptly upon contact with tumor-specific cues. These deviations from healthy tissue can be exploited to trigger payload release specifically inside the tumor mass through the use of stimuli-responsive nanocarriers[17–19]. Among the various triggers, pH responsiveness is the most clinically tractable and has been widely incorporated into polymer-coated nanoparticles bearing acid-labile linkages or protonatable groups[20,21]. Chitosan, a cationic biopolymer rich in primary amine groups (pKa ≈ 6.5), undergoes pH-dependent protonation that swells the polymer matrix in acidic environments and accelerates drug egress, while remaining stable at physiological pH[22]. Conjugation of chitosan with folic acid (FA) further imparts active targeting toward folate-receptor-α-overexpressing tumors, including breast, ovarian and lung carcinomas[23].

Building on these principles, the present study reports the green synthesis of magnetite NPs using *Moringa oleifera* leaf extract, followed by chitosan-folate surface engineering and doxorubicin (DOX) loading. The aim was to fabricate a biocompatible, magnetically responsive and pH-triggered nanocarrier capable of selectively releasing DOX in the tumor microenvironment. We characterized the structural, magnetic and colloidal properties of the system, evaluated its pH-responsive release kinetics under conditions mimicking systemic circulation, the extracellular tumor space and endo-lysosomes, and assessed its in vitro selectivity against MCF-7 breast cancer cells versus normal L929 fibroblasts.

## 2. MATERIALS AND METHODS:

### 2.1 Materials:

Iron(III) chloride hexahydrate ($FeCl_3 \cdot 6H_2O$), iron(II) sulfate heptahydrate ($FeSO_4 \cdot 7H_2O$), low-molecular-weight chitosan (deacetylation degree ≥ 85 %), folic acid (FA), 1-ethyl-3-(3-dimethylaminopropyl)carbodiimide (EDC), N-hydroxysuccinimide (NHS), doxorubicin hydrochloride (DOX·HCl) and 3-(4,5-dimethylthiazol-2-yl)-2,5-diphenyltetrazolium bromide (MTT) were obtained from Sigma-Aldrich (St. Louis, MO, USA). *Moringa oleifera* leaves were collected locally, taxonomically authenticated and shade-dried. Dulbecco's Modified Eagle Medium (DMEM), fetal bovine serum (FBS) and antibiotics were purchased from Gibco (Thermo Fisher, USA). All other reagents were of analytical grade and used without further purification.

### 2.2 Preparation of Moringa oleifera leaf extract

Air-dried leaves were finely powdered, and 10 g of the powder was added to 100 mL of double-distilled water and refluxed at 70 °C for 30 min[11,24]. The cooled extract was filtered through Whatman No. 1 paper, centrifuged at 8000 × g for 10 min and stored at 4 °C until use.

### 2.3 Green synthesis of $Fe_3O_4$ nanoparticles

Magnetite NPs were synthesized using a modified plant-mediated co-precipitation method[12,25,26]. Briefly,

$FeCl_3 \cdot 6H_2O$ and $FeSO_4 \cdot 7H_2O$ were dissolved in deoxygenated water at a 2:1 molar ratio. Twenty-five mL of *M. oleifera* extract was added drop-wise under vigorous mechanical stirring at 60 °C, and the pH of the mixture was raised to 11 with 1 M NaOH. Black precipitates indicating $Fe_3O_4$ formation appeared within minutes. After 2 h of aging, the NPs were collected by an external neodymium magnet, washed three times with ethanol and water, and lyophilized.

### 2.4 Chitosan coating and folic acid conjugation

Chitosan was dissolved in 1 % (v/v) acetic acid (0.5 % w/v), and bare $Fe_3O_4$ NPs were ultrasonically dispersed in this solution for 30 min to allow electrostatic adsorption of the polymer onto the negatively charged oxide surface[22,27]. Folic acid was activated with EDC/NHS (1.2:1.5:1, FA:EDC:NHS) for 1 h in dimethyl sulfoxide and added to the chitosan-coated NPs. The mixture was stirred in the dark for 12 h, after which the FA-CS-$Fe_3O_4$ NPs were collected magnetically and washed to remove unreacted reagents[23,28].

### 2.5 Doxorubicin loading

Drug loading was performed by incubating 10 mg of FA-CS-$Fe_3O_4$ with 2 mg of DOX·HCl in phosphate-buffered saline (PBS, pH 7.4) for 24 h at 4 °C in the dark, under gentle shaking[27,29]. The DOX-loaded NPs were separated magnetically and the unentrapped DOX in the supernatant was quantified spectrophotometrically at 480 nm against a calibration curve. The drug-loading efficiency (DLE) and encapsulation efficiency (EE) were calculated as:

DLE (%) = (mass of loaded DOX / mass of NPs) × 100;

EE (%) = (mass of loaded DOX / mass of initial DOX) × 100.

### 2.6 Physicochemical characterization

UV–Visible absorption spectra were recorded between 200–700 nm. Functional groups were analyzed by FTIR (KBr pellets, 4000–400 $cm^{-1}$). Crystallinity was confirmed by powder X-ray diffraction (Cu-Kα, $2\theta = 10°–80°$). Particle morphology was examined by transmission electron microscopy (TEM) at 200 kV. Hydrodynamic diameter, polydispersity index (PDI) and zeta potential were measured by dynamic light scattering (DLS) using a Zetasizer Nano ZS. Magnetic properties were assessed by vibrating sample magnetometry (VSM) at 300 K[13,30].

### 2.7 In vitro pH-responsive drug release

Drug release was studied by the dialysis-bag method at 37 °C in three media simulating physiological blood (PBS, pH 7.4), the extracellular tumor space (acetate buffer, pH 6.5) and the endo-lysosomal compartment (acetate buffer, pH 5.0)[20,21]. Pre-equilibrated dialysis bags (MWCO 12 kDa) loaded with 5 mg of DOX-FA-CS-$Fe_3O_4$ were immersed in 30 mL of release medium under stirring (100 rpm). At pre-determined intervals, 1 mL of medium was withdrawn for absorbance measurement at 480 nm and replaced with fresh buffer. Each experiment was performed in triplicate.

### 2.8 In vitro cytotoxicity (MTT assay)

MCF-7 (human breast adenocarcinoma) and L929 (mouse fibroblast) cells were maintained in DMEM supplemented with 10 % FBS and 1 % penicillin/streptomycin at 37 °C and 5 % $CO_2$. Cells were seeded into 96-well plates at $1 \times 10^4$ cells/well, incubated for 24 h and exposed to free DOX or DOX-FA-CS-$Fe_3O_4$ at concentrations of 0.5–50 μg $mL^{-1}$ for 48 h. After treatment, MTT solution was added and the formazan absorbance was read at 570 nm[32]. Cell viability and $IC_{50}$ values were calculated relative to untreated controls.

### 2.9 Statistical analysis

All experiments were performed in triplicate (n = 3) and data are expressed as mean ± standard deviation. Comparisons between groups were performed by one-way ANOVA followed by Tukey's post-hoc test using GraphPad Prism v9.0; $p < 0.05$ was considered statistically significant.

## 3. RESULTS

### 3.1 Synthesis and physicochemical characterization

Visual blackening of the reaction mixture within 5 min of NaOH addition indicated the rapid biogenic reduction of iron precursors to magnetite. UV–Vis spectra of the green-synthesized $Fe_3O_4$ showed a characteristic broad absorption between 360–420 nm attributable to magnetite. FTIR spectra revealed Fe–O stretching at 575 $cm^{-1}$, broad –OH/N–H bands centered at 3420 $cm^{-1}$ from chitosan, and additional absorptions at 1605 and 1715 $cm^{-1}$ assigned to the amide carbonyl and carboxyl groups of folic acid, confirming covalent FA-chitosan coupling and

successful surface functionalization. Powder XRD displayed sharp reflections at 2θ = 30.2°, 35.6°, 43.3°, 53.6°, 57.2° and 62.7°, consistent with cubic spinel magnetite (JCPDS 19-0629). The mean crystallite size estimated from the Scherrer equation applied to the (311) reflection was approximately 13.7 nm, in close agreement with the TEM observations and indicating that each particle behaves as essentially a single crystalline domain. TEM micrographs showed quasi-spherical particles with an average core size of 14 ± 3 nm, while VSM gave a saturation magnetization of 52.6 emu $g^{-1}$ with negligible coercivity and remanence, confirming superparamagnetic behavior at room temperature — a property essential both for magnetic targeting and for avoiding magnetically driven aggregation in circulation. Comprehensive parameters are summarized in Table 1.

**Table 1. Physicochemical characteristics of the synthesized nanoparticles (mean ± SD, n = 3).**

| Parameter | $Fe_3O_4$ (bare) | FA-CS-$Fe_3O_4$ | DOX-FA-CS-$Fe_3O_4$ |
|---|---|---|---|
| TEM core size (nm) | 14 ± 3 | 15 ± 4 | 16 ± 4 |
| Hydrodynamic diameter (nm) | 44.8 ± 5.1 | 96.3 ± 6.4 | 134.6 ± 8.2 |
| Polydispersity index (PDI) | 0.18 ± 0.02 | 0.21 ± 0.02 | 0.23 ± 0.03 |
| Zeta potential (mV) | −18.6 ± 1.2 | +34.1 ± 1.4 | +28.4 ± 1.6 |
| Saturation magnetization (emu $g^{-1}$) | 63.4 ± 1.8 | 57.2 ± 1.5 | 52.6 ± 1.3 |
| Drug-loading efficiency, DLE (%) | — | — | 18.7 ± 1.1 |
| Encapsulation efficiency, EE (%) | — | — | 82.4 ± 2.3 |

### 3.2 Hydrodynamic size distribution

DLS profiles (Figure 1) showed a clear stepwise increase in hydrodynamic diameter from 44.8 nm for bare $Fe_3O_4$ to 96.3 nm after chitosan/folate functionalization and 134.6 nm after DOX loading, with all distributions remaining narrow (PDI < 0.25). The shift in zeta potential from negative for bare NPs (−18.6 mV) to highly positive for FA-CS-$Fe_3O_4$ (+34.1 mV) further confirms the coating of protonated chitosan, while the slight reduction after DOX loading (+28.4 mV) reflects partial neutralization by the cationic drug.

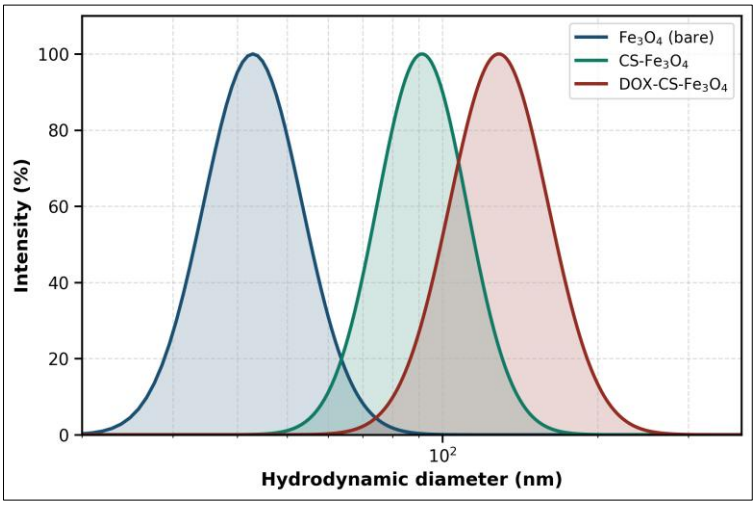


**Figure 1. Intensity-weighted hydrodynamic size distributions (DLS) of bare $Fe_3O_4$, FA-CS-$Fe_3O_4$ and DOX-FA-CS-$Fe_3O_4$ nanoparticles.**

### 3.3 In vitro pH-responsive drug release

The cumulative release of DOX from DOX-FA-CS-$Fe_3O_4$ over 72 h is shown in Figure 2. Release was strongly pH-dependent: at physiological pH 7.4 only 29.1 ± 0.9 % of DOX was liberated, whereas the cumulative release rose markedly to 64.5 ± 1.1 % at the mildly acidic extracellular tumor pH (6.5) and reached 89.8 ± 1.2 % at the endo-lysosomal pH 5.0. An initial burst was observed within the first 8 h at pH 5.0 (~58.7 % release), followed by a slower sustained phase. This profile is consistent with protonation-driven swelling and partial dissociation of the chitosan corona, accompanied by weakening of electrostatic and hydrogen-bond interactions between DOX and the carrier in acidic media.

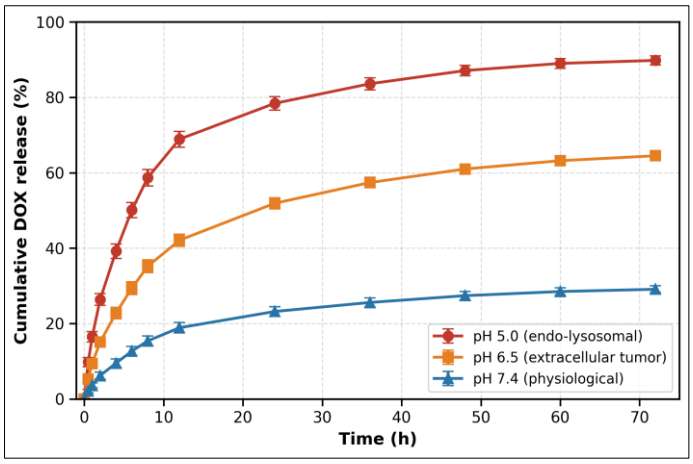


**Figure 2. Cumulative pH-responsive release of doxorubicin from DOX-FA-CS-$Fe_3O_4$ nanoparticles at pH 7.4, 6.5 and 5.0 over 72 h (mean ± SD, n = 3).**

### 3.4 In vitro cytotoxicity and selectivity

Cell viability was concentration-dependent for all treatments (Figure 3). Against MCF-7 cells, DOX-FA-CS-$Fe_3O_4$ was significantly more cytotoxic than free DOX at every concentration tested ($p < 0.05$), reducing viability to 22.8 ± 2.3 % at 10 µg $mL^{-1}$ versus 41.7 ± 3.2 % for free DOX. By contrast, on normal L929 fibroblasts, the nanoformulation preserved 71.5 ± 2.9 % viability at 10 µg $mL^{-1}$, while free DOX dropped viability to 38.4 ± 3.0 %. The corresponding $IC_{50}$ values are summarized in Table 2.

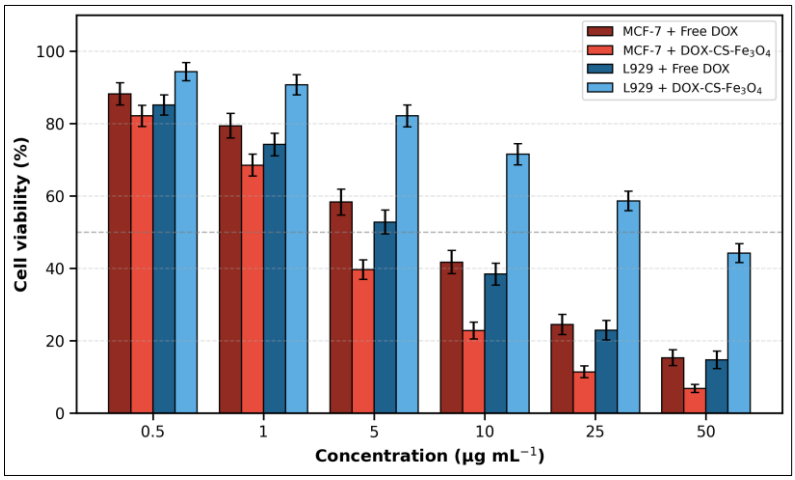


**Figure 3. Cell viability of MCF-7 (cancer) and L929 (normal) cells exposed to free DOX or DOX-FA-CS-$Fe_3O_4$ for 48 h (mean ± SD, n = 3).**

**Table 2. $IC_{50}$ values and selectivity index of free DOX and DOX-FA-CS-$Fe_3O_4$ after 48 h of treatment.**

| Treatment | $IC_{50}$ MCF-7 (µg $mL^{-1}$) | $IC_{50}$ L929 (µg $mL^{-1}$) | Selectivity index* |
|---|---|---|---|
| Blank FA-CS-$Fe_3O_4$ (carrier only) | > 100 | > 100 | — |
| Free DOX | 6.84 ± 0.41 | 7.92 ± 0.46 | 1.16 |
| DOX-FA-CS-$Fe_3O_4$ | 3.42 ± 0.27 | 22.16 ± 1.13 | 6.48 |

**Selectivity index = $IC_{50}$ (L929) / $IC_{50}$ (MCF-7).*

## 4. DISCUSSION

The present work demonstrates that *Moringa oleifera* leaf extract is an efficient green reductant and capping agent for $Fe_3O_4$ nanoparticle synthesis, in agreement with prior reports for biogenic iron oxide systems prepared from *Ruellia tuberosa* and other phytoextracts[12,25]. The polyphenols, flavonoids and ascorbic acid characteristic of *Moringa* are believed to provide both electrons for Fe(III)/Fe(II) reduction and surface anchoring through –OH and –COOH moieties[9,11]. The crystallinity, average core size and saturation magnetization observed here are comparable to those reported for plant-mediated $Fe_3O_4$ systems and are well within the range required for retention

of superparamagnetism, an essential feature for magnetic targeting and MRI-guided therapy[13,14].

A central finding of this study is the strong pH-triggered release behavior of the chitosan-coated platform. The high amine density of chitosan (pKa ≈ 6.5) ensures that the polymer remains relatively compact at pH 7.4 but undergoes extensive protonation, swelling and partial dissolution under acidic conditions, which drives DOX out of the matrix[22,27]. The ~3-fold increase in cumulative release at pH 5.0 versus 7.4 mirrors values reported for other pH-responsive iron oxide-chitosan formulations[20,21,27], and is mechanistically consistent with the dual exploitation of the slightly acidic extracellular tumor space and the more acidic endo-lysosomal compartment after cellular internalization[15,17]. This dual-stage release pattern is desirable because it minimizes premature drug leakage during systemic circulation while maximizing intracellular cytotoxic dosing.

Beyond passive accumulation through the EPR effect[34], conjugation with folic acid endows the carrier with active targeting toward folate receptor-α, which is overexpressed in MCF-7 and many other carcinomas but minimally present on normal tissues[23]. The 2-fold reduction in $IC_{50}$ for DOX-FA-CS-$Fe_3O_4$ against MCF-7 cells compared with free DOX (3.42 vs 6.84 μg $mL^{-1}$), together with the marked increase in $IC_{50}$ on L929 fibroblasts (22.16 μg $mL^{-1}$), translates into a selectivity index of 6.48 — substantially higher than the 1.16 obtained with free drug. Similar improvements have been reported for ZnO and gold-based folate-conjugated nanocarriers[31,35], supporting the generality of receptor-mediated tumor selectivity.

The blank FA-CS-$Fe_3O_4$ carrier was essentially non-cytotoxic up to 100 μg $mL^{-1}$, in line with the favorable safety profile generally reported for biogenic iron oxide and chitosan-based systems[30,37]. The combination of green synthesis, biocompatible polymer corona and TME-responsive release thus addresses several limitations associated with conventional DOX therapy, including off-target cardiotoxicity[29], while leveraging the magnetic responsiveness of the iron oxide core for potential image-guided delivery[14,30].

Several limitations of the current work nevertheless deserve consideration. First, the in vitro nature of the experiments cannot fully recapitulate the complex pharmacokinetics, immune interactions and physical barriers encountered in vivo[33]. Second, only a single tumor cell model (MCF-7) was assessed, and broader studies in folate-receptor-negative lines and in 3D tumor spheroids would help substantiate the receptor-mediated mechanism. Third, while pH responsiveness was confirmed, integration of additional triggers such as redox- or enzyme-responsive linkers may further sharpen tumor specificity through multi-stimuli logic[17,18,36]. Fourth, batch-to-batch reproducibility of biogenic syntheses is intrinsically dependent on the phytochemical composition of plant extracts, which can vary with seasonality, geographic origin and extraction protocol; standardized extracts and quality-control assays of total phenolic and flavonoid content will therefore be a key requirement for any future scale-up[9,10]. These directions, together with comprehensive in vivo biodistribution, magnetic targeting and chronic toxicity studies, will form the basis of follow-up investigations and align with the wider trajectory of nanomedicine toward clinically translatable, intelligent cancer therapeutics[5,38].

## 5. CONCLUSION

A green-synthesized, stimuli-responsive nanocarrier was successfully fabricated by combining *Moringa oleifera*-mediated synthesis of magnetite nanoparticles, chitosan coating, folic acid surface functionalization and doxorubicin loading. The resulting DOX-FA-CS-$Fe_3O_4$ nanoparticles were uniform, superparamagnetic and colloidally stable, and exhibited efficient drug loading (EE 82.4 %). They displayed a pronounced pH-responsive release profile, with ~90 % of DOX released at endo-lysosomal pH 5.0 versus ~29 % at physiological pH, and selectively killed MCF-7 cancer cells while sparing L929 normal fibroblasts (selectivity index 6.48). Three design features converge to deliver this performance: the green synthesis route eliminates toxic reductants and confers an intrinsically biocompatible phytochemical capping layer; the protonatable chitosan corona acts as a smart pH-actuated switch that opens drug egress channels precisely in acidic tumor compartments; and the folate ligand drives receptor-mediated uptake into folate-receptor-overexpressing cancer cells. The proposed system therefore represents a sustainable, biocompatible and tumor-microenvironment-aware platform that meaningfully improves on free doxorubicin in terms of selectivity and triggered intracellular release. Further preclinical validation in animal models, evaluation of magnetically guided accumulation, and exploration of multi-stimuli-responsive variants are warranted to advance such green-engineered nanomedicines toward clinical translation.

## REFERENCES:

1. Sung H, Ferlay J, Siegel RL, Laversanne M, Soerjomataram I, Jemal A, et al. Global Cancer Statistics 2020: GLOBOCAN estimates of incidence and mortality worldwide for 36 cancers in 185 countries. CA Cancer J Clin. 2021;71(3):209–49.

2. Bray F, Laversanne M, Sung H, Ferlay J, Siegel RL, Soerjomataram I, et al. Global cancer statistics 2022: GLOBOCAN estimates of incidence and mortality worldwide for 36 cancers in 185 countries. CA Cancer J Clin. 2024;74(3):229–63.
3. Pérez-Herrero E, Fernández-Medarde A. Advanced targeted therapies in cancer: drug nanocarriers, the future of chemotherapy. Eur J Pharm Biopharm. 2015;93:52–79.
4. Senapati S, Mahanta AK, Kumar S, Maiti P. Controlled drug delivery vehicles for cancer treatment and their performance. Signal Transduct Target Ther. 2018;3:7.
5. Mitchell MJ, Billingsley MM, Haley RM, Wechsler ME, Peppas NA, Langer R. Engineering precision nanoparticles for drug delivery. Nat Rev Drug Discov. 2021;20(2):101–24.
6. Patra JK, Das G, Fraceto LF, Campos EVR, Rodriguez-Torres MDP, Acosta-Torres LS, et al. Nano based drug delivery systems: recent developments and future prospects. J Nanobiotechnology. 2018;16(1):71.
7. Iravani S. Green synthesis of metal nanoparticles using plants. Green Chem. 2011;13(10):2638–50.
8. Singh J, Dutta T, Kim KH, Rawat M, Samddar P, Kumar P. "Green" synthesis of metals and their oxide nanoparticles: applications for environmental remediation. J Nanobiotechnology. 2018;16(1):84.
9. Mittal AK, Chisti Y, Banerjee UC. Synthesis of metallic nanoparticles using plant extracts. Biotechnol Adv. 2013;31(2):346–56.
10. Ahmed S, Ahmad M, Swami BL, Ikram S. A review on plants extract mediated synthesis of silver nanoparticles for antimicrobial applications: a green expertise. J Adv Res. 2016;7(1):17–28.
11. Makarov VV, Love AJ, Sinitsyna OV, Makarova SS, Yaminsky IV, Taliansky ME, et al. "Green" nanotechnologies: synthesis of metal nanoparticles using plants. Acta Naturae. 2014;6(1):35–44.
12. Vasantharaj S, Sathiyavimal S, Senthilkumar P, LewisOscar F, Pugazhendhi A. Biosynthesis of iron oxide nanoparticles using leaf extract of Ruellia tuberosa: antimicrobial properties and their applications in photocatalytic degradation. J Photochem Photobiol B. 2019;192:74–82.
13. Laurent S, Forge D, Port M, Roch A, Robic C, Vander Elst L, et al. Magnetic iron oxide nanoparticles: synthesis, stabilization, vectorization, physicochemical characterizations, and biological applications. Chem Rev. 2008;108(6):2064–110.
14. Wu W, Wu Z, Yu T, Jiang C, Kim WS. Recent progress on magnetic iron oxide nanoparticles: synthesis, surface functional strategies and biomedical applications. Sci Technol Adv Mater. 2015;16(2):023501.
15. Hanahan D, Weinberg RA. Hallmarks of cancer: the next generation. Cell. 2011;144(5):646–74.
16. Gilkes DM, Semenza GL, Wirtz D. Hypoxia and the extracellular matrix: drivers of tumour metastasis. Nat Rev Cancer. 2014;14(6):430–9.
17. Mura S, Nicolas J, Couvreur P. Stimuli-responsive nanocarriers for drug delivery. Nat Mater. 2013;12(11):991–1003.
18. Karimi M, Ghasemi A, Sahandi Zangabad P, Rahighi R, Moosavi Basri SM, Mirshekari H, et al. Smart micro/nanoparticles in stimulus-responsive drug/gene delivery systems. Chem Soc Rev. 2016;45(5):1457–501.
19. Liu D, Yang F, Xiong F, Gu N. The smart drug delivery system and its clinical potential. Theranostics. 2016;6(9):1306–23.
20. Kanamala M, Wilson WR, Yang M, Palmer BD, Wu Z. Mechanisms and biomaterials in pH-responsive tumour targeted drug delivery: a review. Biomaterials. 2016;85:152–67.
21. Liu J, Huang Y, Kumar A, Tan A, Jin S, Mozhi A, et al. pH-sensitive nano-systems for drug delivery in cancer therapy. Biotechnol Adv. 2014;32(4):693–710.
22. Kean T, Thanou M. Biological properties and therapeutic activity of chitosan. Adv Drug Deliv Rev. 2010;62(1):3–11.
23. Low PS, Kularatne SA. Folate-targeted therapeutic and imaging agents for cancer. Curr Opin Chem Biol. 2009;13(3):256–62.
24. Kumar B, Smita K, Cumbal L, Debut A. Biogenic synthesis of iron oxide nanoparticles for 2-arylbenzimidazole fabrication. J Saudi Chem Soc. 2014;18(4):364–9.
25. Rajiv P, Bavadharani B, Kumar MN, Vanathi P. Synthesis and characterization of biogenic iron oxide nanoparticles using green chemistry approach and evaluating their biological activities. Biocatal Agric Biotechnol. 2017;12:45–9.
26. Massart R. Preparation of aqueous magnetic liquids in alkaline and acidic media. IEEE Trans Magn. 1981;17(2):1247–8.
27. Unsoy G, Khodadust R, Yalcin S, Mutlu P, Gunduz U. Synthesis of doxorubicin-loaded magnetic chitosan nanoparticles for pH-responsive targeted drug delivery. Eur J Pharm Sci. 2014;62:243–50.
28. Stella B, Arpicco S, Peracchia MT, Desmaële D, Hoebeke J, Renoir M, et al. Design of folic acid-conjugated nanoparticles for drug targeting. J Pharm Sci. 2000;89(11):1452–64.
29. Tacar O, Sriamornsak P, Dass CR. Doxorubicin: an update on anticancer molecular action, toxicity and novel drug delivery systems. J Pharm Pharmacol. 2013;65(2):157–70.
30. Kandasamy G, Maity D. Recent advances in superparamagnetic iron oxide nanoparticles (SPIONs) for in vitro and in vivo cancer nanotheranostics. Int J Pharm. 2015;496(2):191–218.
31. Patra S, Mukherjee S, Barui AK, Ganguly A, Sreedhar B, Patra CR. Green synthesis, characterization of gold and silver nanoparticles and their potential application for cancer therapeutics. Mater Sci Eng C. 2015;53:298–309.
32. Mosmann T. Rapid colorimetric assay for cellular growth and survival: application to proliferation and cytotoxicity assays. J Immunol Methods. 1983;65(1–2):55–63.
33. Bertrand N, Wu J, Xu X, Kamaly N, Farokhzad OC. Cancer nanotechnology: the impact of passive and active targeting in the era of modern cancer biology. Adv Drug Deliv Rev. 2014;66:2–25.
34. Maeda H, Wu J, Sawa T, Matsumura Y, Hori K. Tumor vascular permeability and the EPR effect in macromolecular therapeutics: a review. J Control Release. 2000;65(1–2):271–84.
35. Anjum S, Hashim M, Malik SA, Khan M, Lorenzo JM, Abbasi BH, et al. Recent advances in zinc oxide nanoparticles (ZnO NPs) for cancer diagnosis, target drug delivery, and treatment. Cancers (Basel). 2021;13(18):4570.
36. Cheng R, Meng F, Deng C, Klok HA, Zhong Z. Dual and multi-stimuli responsive polymeric nanoparticles for programmed site-specific drug delivery. Biomaterials. 2013;34(14):3647–57.
37. Soenen SJ, Rivera-Gil P, Montenegro JM, Parak WJ, De Smedt SC, Braeckmans K. Cellular toxicity of inorganic nanoparticles: common aspects and guidelines for improved nanotoxicity evaluation. Nano Today. 2011;6(5):446–65.
38. Jurj A, Braicu C, Pop LA, Tomuleasa C, Gherman CD, Berindan-Neagoe I. The new era of nanotechnology, an alternative to change cancer treatment. Drug Des Devel Ther. 2017;11:2871–90.